# Multiple substitutions of methionine 129 in human prion protein reveal its importance in the amyloid fibrillation pathway

Nystrom, Sofie ; Mishra, Rajesh ; Hornemann, Simone ; Aguzzi, Adriano ; Nilsson, K Peter R ; Hammarstrom, Per

Abstract: The role of the polymorphism 129M/V in the human prion protein is well documented regarding disease susceptibility and clinical manifestations. Little is however known about the molecular background to this phenomenon. We herein investigated the conformational stability, amyloid fibrillation kinetics and seeding propensity of different 129-mutants, located in  -strand 1 of PrP (129M (wt), 129A, 129V, 129L, 129W, 129P, 129E, 129K and 129C) in HuPrP90-231. The mutations 129V, 129L, 129K and 129C did not affect stability (midpoints of thermal denaturation, Tm =65-66 °C), whereas the mutants 129A and 129E and the largest side chain 129W were destabilized by 3-4 °C. The most destabilizing substitution was 129P which lowered the Tm by 7.2 °C. All mutants, except 129C, formed amyloid like fibrils within hours during fibril formation under near physiological conditions. Fibril forming mutants, showed a sigmoidal kinetic profile and showed shorter lag times during seeding with preformed amyloid fibrils implicating a nucleated polymerization reaction. In the spontaneous reactions, the lag time of fibril formation was rather uniform for the mutants 129A, 129E, 129V, and 129L resembling the wild type 129M. When the substituted amino acid had a distinct feature discriminating it from the wild type, such as size (129W), positive charge (129K) or rotational constraint (129P), the fibrillation was impeded. 129C did not form ThT/Congo red positive fibrils and non-reducing SDS PAGE of 129C during fibrillation conditions at different time points revealed covalent dimer formation already 15 minutes after fibrillation reaction initiation. Position 129 appears to be a key site for dictating PrP receptiveness towards recruitment into the amyloid state.

DOI: https://doi.org/10.1074/jbc.M112.372136

JBC Papers in Press. Published on June 5, 2012 as Manuscript M112.372136
The latest version is at http://www.jbc.org/cgi/doi/10.1074/jbc.M112.372136



# Multiple substitutions of Methionine 129 in Human Prion Protein Reveal its Importance in the Amyloid Fibrillation Pathway

**Sofie Nyström[1], Rajesh Mishra[1], Simone Hornemann[2], Adriano Aguzzi[2], K. Peter R. Nilsson[1] and Per Hammarström[1]**

[1]IFM-Department of Chemistry, Linköping University, SE-581 83 Linköping, Sweden, [2]Institute of Neuropathology, University Hospital of Zurich, CH-8091 Zurich, Switzerland

**Running title: Mutations in position 129 of the human prion protein*

To whom correspondence should be addressed: Per Hammarström, IFM-Kemi, Linköping University, S-581 83 Linköping, Sweden, Tel: +4613285690, Fax +4613281399, Email: perha@ifm.liu.se

**Keywords:** amyloidogenesis; recombinant HuPrP; polymorphism; amino acid substitutions; dimerization

**Background**: A polymorphism in position 129 in the human prion protein modulates susceptibility to prion infection and disease phenotype.
**Results**: Mutations to various amino acids highlights the importance of position 129 during amyloid fibrillation.
**Conclusion**: Position 129 is a key site for early intermolecular interactions during fibrillation.
**Significance**: Insight into early mechanisms of aggregation implicates a means to prevent fibrillation

## SUMMARY

**The role of the polymorphism 129M/V in the human prion protein is well documented regarding disease susceptibility and clinical manifestations. Little is however known about the molecular background to this phenomenon. We herein investigated the conformational stability, amyloid fibrillation kinetics and seeding propensity of different 129-mutants, located in β-strand 1 of PrP (129M (wt), 129A, 129V, 129L, 129W, 129P, 129E, 129K and 129C) in $HuPrP_{90-231}$. The mutations 129V, 129L, 129K and 129C did not affect stability (midpoints of thermal denaturation, $T_m$ =65-66 °C), whereas the mutants 129A and 129E and the largest side chain 129W were destabilized by 3-4 °C. The most destabilizing substitution was 129P which lowered the $T_m$ by 7.2 °C. All mutants, except 129C, formed amyloid like fibrils within hours during fibril formation under near physiological conditions. Fibril forming mutants, showed a sigmoidal kinetic profile and showed shorter lag times during seeding with preformed amyloid fibrils implicating a nucleated polymerization reaction. In the spontaneous reactions, the lag time of fibril formation was rather uniform for the mutants 129A, 129E, 129V, and 129L resembling the wild type 129M. When the substituted amino acid had a distinct feature discriminating it from the wild type, such as size (129W), positive charge (129K) or rotational constraint (129P), the fibrillation was impeded. 129C did not form ThT/Congo red positive fibrils and non-reducing SDS PAGE of 129C during fibrillation conditions at different time points revealed covalent dimer formation already 15 minutes after fibrillation reaction initiation. Position 129 appears to be a key site for dictating PrP receptiveness towards recruitment into the amyloid state.**

The prion protein (PrP) is most abundant in mammalian neurons but is ubiquitously expressed throughout various cells and tissues. The functional role of native PrP is not fully understood. PrP is associated with a number of different prionoses, both sporadic, inherited and acquired, all of which are invariably fatal. The common molecular pathognomonic marker for prionoses is the presence of severe vacuolation within the CNS rendering a sponge like tissue. Concomitant with the presence of spongiosis is the presence of a conformational isoform of PrP, which has converted from a largely helical

globular protein $PrP^{C}$ that misfold into an aggregation prone beta-sheet conformation, $PrP^{Sc}$, that often assemble into protein deposits with conspicuous similarities to amyloid (1).

Several inherited prion disease-causing point mutations are found in the human PrP gene (PRNP) (2,3). There are also two nonpathogenic polymorphisms, methionine or valine in position 129 (M129V) and glutamic acid or lysine at codon 219 (E219K) (4,5). These polymorphisms are not directly pathogenic but on the contrary hetrozygosity at either of these positions is associated with resistance to sporadic Creutzfeldt-Jakob disease (sCJD) (6,7). The polymorphism in position 129 is also associated with sporadic Creutzfeldt-Jakob disease phenotype and influences the molecular type of prion strains (8). Furthermore, differences in codon 129 determine the phenotype of patients suffering pathogenic mutations elsewhere in the PRNP gene (9-13). Homozygous individuals are more susceptible to acquired prion disease such as Kuru, variant CJD and iatrogenic CJD (14-19).

Taken together there is ample evidence that position 129 in PrP is a key site for prion disease susceptibility and hence most likely for PrP misfolding. The effect of the natural polymorphism at position 129 has been studied in vitro in several studies regarding both amyloid fibrillation kinetics and oligomerization. Reorganization of $HuPrP_{90-231}$ into mature amyloid fibrils under denaturing conditions is enhanced if position 129 encodes a valine while methionine in this position favors formation of soluble oligomers (20-22).

Amyloid fibril formation is a multiordered, nucleation dependent process (23). Because nucleation is a multiorder reaction its rate especially at low protein concentrations should be stochastic. This feature is reflected by a time variation of the lag phase of fibril formation (24). During amyloidogenesis, the fibril elongates through monomer addition and conversion and in addition the fibril is fragmented leading to multiplication of fibril elongation sites. It is hence evident that fragmentation of amyloid fibrils is of great importance for fibril replication. The rate of the growth phase is a measure of fibril fragility rather than of cooperativity in monomer addition (25-27).

The amyloid formation pathways of many proteins involve formation of oligomeric species. These oligomers comprise varying numbers of non-native protein molecules, but most often they do not display the features of amyloid regarding ThT fluorescence. It has been shown that oligomers of many proteins involved in neurodegenerative diseases are the most toxic species in cell culture (28,29) including the prion protein (30,31). PrP forms oligomers via different pathways giving rise to different distinctly different oligomers from the same primary structure (32). The formation of different oligomers can also be modulated by the polymorphism in position 129. The propensity to form oligomers and the properties of the oligomers are not affected by the polymorphism, but the stacking of oligomers was suggested to be aggravated by the valine residue (33).

In our current study we elucidated the conformational stability and amyloid propensity of recombinant $HuPrP_{90-231}$ with variations in position 129. We made use of the range of properties offered by amino acid substitution. To investigate the role of increasing number of methyl groups, alanine, valine and leucine were used. To elucidate the role of the sulfur atom in the wild type methionine, cysteine was included in the study. Lysine and glutamic acid should give information on the involvement of electrostatic interactions. Tryptophan was employed to examine influence of bulkiness. Proline was used to investigate how rotational constraint influences amyloid formation.

## EXPERIMENTAL PROCEDURE

*Expression and Purification of $HuPrP_{90-231}$ and $HuPrP_{121-231}$* - Plasmids (pREST A) containing HuPrP wt (129M) genes of desired lengths were obtained from K. Wüthrich (34). Site directed mutagenesis was performed using the QuikChange mutagenesis kit (Stratagene, La Jolla, CA, USA) according to manufacturer's guide lines and mutants were verified by DNA sequencing (GATC biotechnology, Konstanz, Germany). The plasmids were transformed into BL21/DE3 cells and were grown on plates overnight. The cells were transferred to 1.5 l Terrific Broth (MP biochemicals) supplemented with 100 µg/ml ampicillin at 37ºC with shaking. At $OD^{600}$~2.5 isopropyl β-D-galactopyranoside was added to a final concentration of 1.5 mM to induce protein production. Agitation at 37 ºC was maintained during protein expression and cells were harvested by centrifugation after overnight induction, the

pellet was resuspended in buffer G (6 M guanidine hydrochloride, 10 mM Tris-HCl, pH 8.0, 100 mM Na2PO4, 10 mM reduced glutathione) and frozen at -80ºC until needed.

After thawing, sonication and centrifugation, the soluble fraction was added to Ni-NTA-agarose (Qiagen) in a disposable column (3 ml). The agarose was washed with 10 ml buffer G, 7 ml 50% buffer G and 50% buffer B (10 mM Tris-HCl, 100 mM $Na_2PO_4$, pH 8.0), 5 ml Buffer B and finally 5 ml Buffer B supplemented with 50 mM imidazole. The protein was eluted using 10 ml Buffer E (10 mM Tris-HCl, 100 mM $Na_2PO_4$, 500 mM imidazole pH 5.8). The washing procedure was repeated until the elution fractions no longer contained protein detectable by the Bradford assay (BioRad). The elution fractions were pooled, concentrated and applied to a Hiload 16/60 superdex 75 prep grade column (GE Healthcare) using a BioLogic LP system (BioRad) with a continues flow rate of 1 ml/min. Buffer F (50 mM phosphate (pH 7.4), 100 mM NaCl, 50 mM KCl) was used for running buffer. Purity of obtained proteins was confirmed by SDS-PAGE (35) . All described experiments with PrP were conducted in a biosafety P3** facility.

*CD spectroscopy* - A Chirascan CD spectrometer (Applied photophysics) and 1 mm cuvette was used for all measurements. Far UV spectra between 195 and 250 nm were measured at 4 ºC to assess the native protein structure. Thermal denaturation was monitored by recording the molar ellipticity at 222 nm while the sample was heated from 4 ºC to 90 ºC at 1 º/min. The sample was cooled down and the far UV spectrum was again measured at 4 ºC for the refolded protein. The respective $T_m$ was calculated according to John et al (36).

*Amyloidogenesis of HuPrP under near native conditions* **-** The protein was diluted in buffer F to the desired concentration (6 µM), ThT was added to a concentration of 2 µM and the protein solution was aliquoted (100 µl) into the wells of microtiter plates (costar NT 96 well, black with clear bottom, Corning, USA). The plate was sealed with sealing tape. Typically 6 identical samples were prepared for each fibrillation experiment. The plate was shaken in a Tecan SafireII plate reader at high speed in linear mode. Every 15 minutes the shaking was halted and fluorescence intensity was measured form the bottom of the plate by excitation at 440 nm and emission at 480 nm. Kinetic traces were fitted according to Almstedt et al (35), 2009, to obtain the lag-phase and the growth rate for each trajectory. Statistical analysis comparing experiments were performed using unpaired two tailed t-test using GraphPad Prism 5 sofware. A p-value $<0.05$ was considered significant.

*Polarization microscopy* - Congo red for microscopy analysis was added to mature fibrils in solution at a molar ratio of fibril:dye 3:1. Stained fibrils were left to self-sediment over night at 4 ºC. The supernatant was removed and the pelleted fibrils were transferred to superfrost plus glass slides (Thermo Fisher, Walldorf, Germany), covered with Mounting medium (Dako, Glosrup, Denmark) and cover glass was sealed with transparent nail polish. Congo Red stained samples were analysed using a Nikon light microscope equipped with polarizers for both incoming light and in front of the detector.

## RESULTS

*Conformational stability of native $HuPrP_{90-231}$ 129 mutants* - The conformation of the native $HuPrP_{90-231}$ protein variants was monitored by far-UV CD spectroscopy. All variants displayed a spectrum with two negative peaks at 222 and 208 nm followed by a positive peak at wavelengths below 200 nm (Fig 1a). These features are consistent with native folded PrP dominated by α–helical structure and is in agreement with spectra in the literature (37). The thermodynamic stability of the protein variants was thereafter monitored by far-UV CD spectroscopy. Spectra were recorded at 4 ºC, followed by sequential steps of thermal denaturation monitored at 222 nm. After complete denaturation at 90 ºC, the sample was cooled to 4 ºC and far-UV CD spectra were recorded again to assess any irreversible change of secondary structure upon one unfolding-refolding cycle.

All mutants except 129P showed similar far UV CD spectra before denaturation (Fig. 1a). 129P displayed decreased positive amplitude between 195 and 200 nm compared to wt PrP, with a concomitant shift of the peak towards 197 nm indicating loss of helical structure (38). The thermal stability curves of all mutants showed a sloping pre-transitional baseline followed by a cooperative thermal unfolding transition. Comparing the thermal stability of the mutants

showed that the 129M, 129V, 129L, 129K and 129C were the most stable and all within error showed $T_m$'s of 65-66 °C (Fig 1b, Table 1). The 129A, 129E and 129W mutants were destabilized by 3-4 °C and 129P was the most destabilized mutant with a $T_m$ lowered by 7.2 °C. After thermal denaturation refolding was allowed at 4 °C and the reversibility of the thermal unfolding was compared. Interestingly the spectral feature of 129P described above at 197 nm also appeared in the spectra for 129W and 129E and, to some extent, 129A (Fig. 1c) after refolding. The 129P, 129W, 129E and 129A mutants were also the most destabilized mutants and the amplitude of the irreversibility at 195-200 nm correlated well with the respective $T_m$. Traditionally the amount of α–helix and reversibility of helical structure is easily assessed at 222 nm. The reversibility of the CD signal at 222 nm for 129C and 129W showed the largest difference between the pre-denaturation and post-denaturation spectra (Fig 1c), corroborating the spectral findings discussed above in the 195-200 nm region. The difference in molar ellipticity at 222 nm in the spectrum before and after thermal denaturation was between 9-12 % for stable variants and 15-22 % for mutants with lower $T_m$-values. One of the most stable variants, 129C, also displays the largest loss of helical structure upon refolding. This mutant lost 30% of its helical structure upon thermal denaturation-refolding (Table 1).

As a reference for the CD measurements the shorter variant $HuPrP_{121-231}$ (129M) comprising only the folded globular domain was employed. Comparing the shorter 121-231 construct and longer 90-231 construct ($HuPrP_{90-231}$), the native spectrum, the $T_m$ and the reversibility was indistinguishable within error for these parameters (Table 1), but did reveal a more cooperative thermal transition compared to the longer construct (Fig 1b). Nevertheless, the identical $T_m$ rules out strong interactions between the globular domain 121-231 with the unstructured partial N-terminal 90-120 domain on the folding properties of $HuPrP_{90-231}$ in this assay.

*Amyloid fibril formation of HuPrP 129 mutants* - Previously we have described in detail that vigourous shaking of natively folded PrP in 2 mL cryotubes induced protein aggregation and amyloidogenesis, in physiological buffer at 37 ˚C (35). Aggregates produced according to this protocol were collected after 7 h of agitation, stained with Congo red and placed on glass slides. Imaging with a polarization microscope revealed that all mutants except for 129C formed Congo red stained birefringent aggregates indicating the presence of symmetric Congo red binding sites, the tinctorial hallmark of amyloid fibrils (Fig 2a). The aggregates of all mutants except for 129C were also positive for ThT fluorescence following excitation at 440 nm with an emission peak at 485 nm, which was absent for native protein (Fig. 2b). The ThT fluorescence intensity of the fibrils varied depending on mutant (Table 2).

*Nonreducing SDS-PAGE of 129C* - The lack of correlation between thermal stability and refolding capability together with the inability to form Congo Red and ThT positive fibrils of 129C led us to investigate if this was due to intermolecular disulfide formation. Aliquots from fibrillation reactions of 129M and 129C were collected at 0 min, 15 min, 2 hours and 4 hours. Samples were boiled in non-reducing SDS containing sample loading buffer and loaded on SDS-PAGE gels followed by Coomassie staining. The 129M variant displayed distinct monomeric band during the monitored time course. In the case of 129C, a dimeric protein was present already at the initial time point. As fibrillation proceeded, the monomeric band faded and the dimeric band was enhanced (Fig 3). At the end of the time course, a faint tetrameric band could also be observed. Dimer formation should be caused by intermolecular disulfide formation between cysteine residues at position 129.

*Amyloid fibrillation kinetics* - Formation of amyloid fibrils of HuPrP under near physiological conditions was monitored by measuring ThT fluorescence intensity during the fibrillation process in a 96 well plate format. Six separate samples of identical composition were used for each PrP variant. Every individual trace showed a characteristic lag, growth and equilibrium trajectory (Fig. 4a, red lines). This is consistent with the notion that the amyloid fibrillation process of PrP is a nucleation dependent polymerization reaction. The ensembles of individual mutant trajectories of identical samples revealed that the protein showed a rather variable lag-phase indicating that PrP fibrillation kinetics is a process with a stochastic component which appeared to be mutation dependent. This notion is consistent with

previous data showing an initial aggregation reaction preceding fibril formation which renders a kinetic trap from which fibrils protrude (35). This is the background for the variations noted in the fibrillation trajectories. Lag times for all mutants are listed in Table 3. Comparing lag times during the spontaneous fibril formation reaction the wildtype-like mutants (129A, 129V and 129L) were within the same interval as 129M (~5 h) (Fig 4a, b, Table 3). Substitutions to conformationally constrained proline, bulky tryptophan or charged residues (glutamic acid and lysine) substantially elongated the lag time of amyloid formation (Fig 4b, Table 3). The 129C mutant did not form ThT positive fibrils within the time course of the experiment (Fig 4a, note the different y-axis, Table 3).

The growth phase of the fibril formation trajectories was defined as the slope of the ThT fluorescence following the end of the lag-phase to half the normalized maximum ThT intensity for each trajectory (35). In the amyloid fibril formation reactions the highest mean growth rates were obtained for 129M and 129A. The clinically relevant mutant 129V, known to prolong incubation time of prion disease in heterozygote carriers and even protect against prion infection, had a slower growth rate than the wild type (129M) protein (Fig 4a, b, Table 3), ($p<0.0001$) on par with 129W, 129K and 129E.

*The effect of seeding* - To investigate the seeded fibrillation reactions, 1% seed from previous fibrillation reactions were added to fresh protein and the fibrillation kinetics was monitored using the same setup and analyzing the same parameters as for the spontaneous reaction.

Seeding of the mutants with preformed fibrils of the same sequence efficiently shortened the lag time for the129M/A/L/V/W/P/E variants (Fig 4a, black traces). The lag time of the 129K mutant was unaffected by seeding (Fig 4a,b, Table 3). Addition of seed did however induce all samples (6/6) to convert into ThT positive fibrils within the monitored time frame, whereas only 3/6 samples converted spontaneously (Fig 4a,b, Table 3). The 129C mutant which did not form ThT fluorescent fibrils was also unaffected by seeding with 1% 129C protein subjected to a previous round of fibril formation conditions (Fig 4a, note the different y-axis, Table 3). Interestingly, addition of 1 % seed from preformed wild type fibrils (129M) did induce formation of ThT positive fibrils of 129C on the same time scale as the wild type protein itself (Fig 4a inset). The strongest seeding effect was observed for the 129W and 129P mutants and the least affected mutant in terms of lag time (129K excluded) was 129V (Fig. 4b). Seeding of 129W also showed a prominent effect on the growth rate of amyloid formation whereas the growth rates for the rest of the studied mutants were only modestly affected (Fig 4b, Table 3).

## DISCUSSION

Misfolding of $PrP^{C}$ into $PrP^{Sc}$ in the prionoses frequently entails the accumulation of PrP aggregates with compelling similarities to amyloid deposits formed in local and systemic amyloidoses. High resolution structural models of $PrP^{Sc}$ have been presented (39). In two models the $PrP^{C}$ molecule is partially refolded starting from the unstructured segment (from 90, or 114) up to position 175. The PrP molecules are herein arranged in intermolecular β–sheet configurations (β -helical or spiral), comprising trimeric building blocks(40,41). The C-terminal helical domain is to a large extent intact in these models. On the contrary, there are other more dramatic structural rearrangements of misfolded PrP proposed by the Surewicz group. Herein, the PrP sequence including 90-231 has been shown to be essentially completely misfolded *in vivo* in prion infected mice as deduced by hydrogen deuterium exchange kinetics (42) into an in-register parallel cross-β–sheet amyloid state. The structural differences between these models and the evidence that deposited PrP is conformationally diverse within distinct prion strains(43), implicates that aggregated PrP is polymorphic. Therefore several positions within the PrP sequence should influence $PrP^{Sc}$ structure and $PrP^{C}$ conversion. In the human prion protein the 129 position has been shown to constitute the most prevalent single residue linked to prion pathogenesis and is known to be polymorphic for either M or V. These substitutions in position 129 also modulate the $HuPrP_{90\text{-}231}$ amyloidogenicity under near physiological conditions *in vitro*. The Surewicz group has reported that 129V and M have the same fibril formation kinetics when subjected to mildly denaturing conditions (44). In that study the 129M/V variants did not fibrillate under native conditions when the agitation was slow, in

accordance with our previous report on stagnant incubation of $HuPrP_{90-231}$ (129M) (35). Nevertheless, studies of the D178N mutation in context with either 129M or 129V showed faster fibrillation rates both regarding a shorter lag phase and faster growth rate when in context with 129M (44). This observation is consistent with our data on 129M/V in this paper (Table 3), where the growth rate for 129V was slower compared to 129M both for unseeded ($0.11 \pm 0.06$ $h^{-1}$ vs $0.37 \pm 0.11$ $h^{-1}$) and for self-seeded reactions ($0.11 \pm 0.02$ $h^{-1}$ vs $0.44 \pm 0.09$ $h^{-1}$) ($p<0.0001$). In addition the lag time for self-seeded 129M ($1.5 \pm 0.2$ h) compared to self-seeded 129V ($2.9 \pm 1.0$ h) was significantly faster ($p<0.005$).

We have herein compared the amyloidogenicity and conformational stability of nine different recombinant $HuPrP_{90-231}$ sequences with substitutions in position 129 (including M/V) to investigate its possible effect on misfolding of the protein into the amyloid-like state under near native conditions.

The conformational stability of the 129V, 129L, 129K and 129C mutations were all within error indistinguishable from the wt 129M protein. The 129A, 129E, 129P and 129W mutants were less stable than wt. A possible correlation for the destabilization as a consequence of side chain were found when comparing the influence on stability with the apolar size of the side chain compared to the wt 129M (Table 1). Influence of the unstructured 90-120 sequence, which has been reported to become structured at neutral pH, was found to be very low because of indistinguishable conformational stability of the $HuPrP_{121-231}$ and the $HuPrP_{90-231}$ variants. The most severely destabilizing mutation was 129P which decreased the stability by 7.2 °C. This observation is consistent with beta-sheet breaker propensity of proline showing that beta-strand 1 is rather important for PrP stability. To obtain a reference to exemplify the magnitude of destabilization of substitutions in position 129 we compared the stability results with two previously reported highly destabilized disease mutants associated with inherited prionoses: H187R (45) and F198S (46). When analyzed under the exact same conditions in the context of $HuPrP_{90-231}$ the H187R/129M mutant had a $T_m$ of 53.2±0.6 °C and F198S/129M had a $T_m$ of 48.6±0.3 °C providing $\Delta T_m$:s as compared to wt by 12.4 °C and 17.0 °C respectively (Table 1). Hence the 129P mutation, although substantial, is less destabilizing than these highly destabilized naturally occurring pathogenic mutations.

Congo red birefringence and ThT fluorescence showed that eight highly diverse 129-mutants formed amyloid fibrils under the conditions used herein (intense agitation of folded PrP in physiological buffer, at 37 ˚C). In the kinetic trajectories (ThT assay) the fibril conversion competent mutants showed a lag phase followed by a rather steep growth phase which ended in an equilibrium phase at the end of the reaction. This behavior indicated that the protein regardless of substitution in the 129 position displayed nucleated polymerization kinetics. This was especially evident when the amyloid fibril formation reactions were run in the presence of 1% preformed PrP fibrils as seeds, which rather consistently shortened the lag times. A schematic model of the fibril formation reactions is presented in Fig 5. Spontaneous fibril formation (Fig. 5 i) is initiated by dimerization followed by aggregation into oligomeric aggregates that slowly convert to amyloid fibrils (35). Fibril seeds added to a new fibrillation reaction (Fig. 5 ii) renders direct addition and rapid conversion of monomeric PrP.

In stark contrast to the other eight variants in position 129, 129C completely resisted spontaneous conversion into amyloid fibrils. Investigation of this mutant by non-reducing SDS-PAGE suggests that this is due to an intermolecular disulfide bond formation very early in the nucleation process (Fig 3). This, in turn, abrogates further nucleation and fibrillation of this mutant (Fig 5 iv). Addition of preformed seeds from the 129M sequence, however, expediently enabled formation of ThT positive fibrils from 129C sequence. This shows that the wild type seeds are able to recruit 129C monomers and convert them into the amyloid conformation, hence diverting 129C out of the kinetic trap introduced by covalent dimerization and places 129C on the seeded conversion track (Fig. 5 ii). Importantly, dimerization has been shown to be the rate determining step in amyloid fibril conversion of mPrP albeit under different conditions compared to those used in our study (47). Interestingly a dimer model within a crystallization interface where the beta-stand 1 was paired in an antiparallel configuration between two PrP monomers in a co-crystal complex with an antibody has been

reported (48) (Fig 6). This observation supports that beta-stand 1 has propensity for inducing dimerization of PrP in the native state. Our data suggests that this state, if locked in this conformation, would be a conversion incompetent state. We base that conclusion on all the other conversion competent 129 mutations in our study. That dramatic conformational reorganization of the C-terminal domain follows initial dimerization has been shown by structural studies of recombinant PrP amyloid fibrils (49) and studies of PrP mutants with intramolecular disulfide cross-links within the C-terminal domain that efficiently inhibited fibril formation (50). Albeit these studies observed PrP fibrils formed under denaturing conditions the latter study proposes the building block of mPrP fibrils to be composed of domain swapped dimers.

In the spontaneous reaction the lag time of fibril formation was rather consistent for all wild type-like mutants (129A, 129V, 129L). Residues with special features like bulkiness (129W), rotational constrain (129P) and charge (129E and 129K) displayed longer lag times. We speculate that the initial aggregation/oligomerization step of the conversion reaction is affected by the 129W mutation by heightening the barrier of the conformational conversion from the oligomeric aggregate to amyloid fibril (step 3 in Fig 5 i). The pronounced seeding efficiency for the 129W mutation strengthens this hypothesis, because this trap is circumvented. The 129P mutant showed a highly variable lag phase in the spontaneous reactions which could reflect different conformational populations of proline cis-trans isomers during the initial dimerization and aggregation steps (steps 1-2 in Fig 5a). The 129K mutant displayed an indifferent lag time when seeded, but increased the conversion ratio (Table 3). This observation in combination with the notion that glutamic acid in this position drastically shortens the lag time during seeding makes us conclude that positive charge – charge repulsions in the intermolecular interface of initial aggregation is contributing to this alteration and hence follows an alternate route of association and conversion (step 7 in Fig 5 iii). Hence, the recruitment of native monomer to the nuclei appears abrogated by positive-charge repulsion caused by charged residues exposed on the surface of the fibrillation competent conformation. The seeding mechanism is distorted. The spontaneous reaction is also retarded by positive charge repulsion. This positive charge repulsion effect is indirectly supported by previous reports on poly-anion (DNA, RNA, GAG, and LCP) modulation of PrP fibril formation and $PrP^{C}$ to $PrP^{Sc}$ conversion (51-56)).

Formation of intermolecular disulfides in the 129C variant was an early event in aggregation and fibrillation (Fig. 5 iv). Hence, arresting the native PrP conformation by antiparallel locking of two monomers at beta-stand 1 is putatively a strategy for intervention of PrP misfolding. The extent of the dimerization interface is unlikely to be limited to beta-strand 1, but could involve an extended portion of PrP. This is currently being investigated in our laboratories. Nevertheless, given that a high resolution target for an antiparallel arrangement of beta-stand 1 in a native state dimer interface was suggested by recent X-ray crystallography data, (48) (Figure 6) this could be an exploitable avenue for classical drug discovery endeavors. Similar small molecule kinetic stabilization of the native state has fruitfully been exploited to avoid misfolding of the tetrameric protein transthyretin (57,58)

**REFERENCES**

1. Cobb, N. J., and Surewicz, W. K. (2009) *Biochemistry* **48**, 2574-2585
2. Collinge, J. (2001) *Annual review of neuroscience* **24**, 519-550
3. Mead, S. (2006) *Eur J Hum Genet* **14**, 273-281
4. Owen, F., Poulter, M., Collinge, J., and Crow, T. J. (1990) *Nucleic acids research* **18**, 3103
5. Petraroli, R., and Pocchiari, M. (1996) *American journal of human genetics* **58**, 888-889
6. Palmer, M. S., Dryden, A. J., Hughes, J. T., and Collinge, J. (1991) *Nature* **352**, 340-342
7. Shibuya, S., Higuchi, J., Shin, R. W., Tateishi, J., and Kitamoto, T. (1998) *Lancet* **351**, 419

8. Polymenidou, M., Stoeck, K., Glatzel, M., Vey, M., Bellon, A., and Aguzzi, A. (2005) *Lancet neurology* **4**, 805-814
9. Dlouhy, S. R., Hsiao, K., Farlow, M. R., Foroud, T., Conneally, P. M., Johnson, P., Prusiner, S. B., Hodes, M. E., and Ghetti, B. (1992) *Nature genetics* **1**, 64-67
10. Goldfarb, L. G., Petersen, R. B., Tabaton, M., Brown, P., LeBlanc, A. C., Montagna, P., Cortelli, P., Julien, J., Vital, C., Pendelbury, W. W., and et al. (1992) *Science (New York, N.Y* **258**, 806-808
11. Poulter, M., Baker, H. F., Frith, C. D., Leach, M., Lofthouse, R., Ridley, R. M., Shah, T., Owen, F., Collinge, J., Brown, J., and et al. (1992) *Brain* **115 ( Pt 3)**, 675-685
12. Monari, L., Chen, S. G., Brown, P., Parchi, P., Petersen, R. B., Mikol, J., Gray, F., Cortelli, P., Montagna, P., Ghetti, B., and et al. (1994) *Proceedings of the National Academy of Sciences of the United States of America* **91**, 2839-2842
13. Hainfellner, J. A., Parchi, P., Kitamoto, T., Jarius, C., Gambetti, P., and Budka, H. (1999) *Annals of neurology* **45**, 812-816
14. Collinge, J., Palmer, M. S., and Dryden, A. J. (1991) *Lancet* **337**, 1441-1442
15. Collinge, J., Beck, J., Campbell, T., Estibeiro, K., and Will, R. G. (1996) *Lancet* **348**, 56
16. Zeidler, M., Stewart, G., Cousens, S. N., Estibeiro, K., and Will, R. G. (1997) *Lancet* **350**, 668
17. Hill, A. F., Butterworth, R. J., Joiner, S., Jackson, G., Rossor, M. N., Thomas, D. J., Frosh, A., Tolley, N., Bell, J. E., Spencer, M., King, A., Al-Sarraj, S., Ironside, J. W., Lantos, P. L., and Collinge, J. (1999) *Lancet* **353**, 183-189
18. Lee, H. S., Brown, P., Cervenakova, L., Garruto, R. M., Alpers, M. P., Gajdusek, D. C., and Goldfarb, L. G. (2001) *The Journal of infectious diseases* **183**, 192-196
19. Mead, S., Stumpf, M. P., Whitfield, J., Beck, J. A., Poulter, M., Campbell, T., Uphill, J. B., Goldstein, D., Alpers, M., Fisher, E. M., and Collinge, J. (2003) *Science (New York, N.Y* **300**, 640-643
20. Lewis, P. A., Tattum, M. H., Jones, S., Bhelt, D., Batchelor, M., Clarke, A. R., Collinge, J., and Jackson, G. S. (2006) *The Journal of general virology* **87**, 2443-2449
21. Baskakov, I., Disterer, P., Breydo, L., Shaw, M., Gill, A., James, W., and Tahiri-Alaoui, A. (2005) *FEBS letters* **579**, 2589-2596
22. Tahiri-Alaoui, A., Gill, A. C., Disterer, P., and James, W. (2004) *The Journal of biological chemistry* **279**, 31390-31397
23. Cohen, S. I., Vendruscolo, M., Dobson, C. M., and Knowles, T. P. (2012) *Journal of molecular biology*
24. Hortschansky, P., Schroeckh, V., Christopeit, T., Zandomeneghi, G., and Fandrich, M. (2005) *Protein Sci* **14**, 1753-1759
25. Collins, S. R., Douglass, A., Vale, R. D., and Weissman, J. S. (2004) *PLoS biology* **2**, e321
26. Xue, W. F., Homans, S. W., and Radford, S. E. (2008) *Proceedings of the National Academy of Sciences of the United States of America* **105**, 8926-8931
27. Knowles, T. P., Waudby, C. A., Devlin, G. L., Cohen, S. I., Aguzzi, A., Vendruscolo, M., Terentjev, E. M., Welland, M. E., and Dobson, C. M. (2009) *Science (New York, N.Y* **326**, 1533-1537
28. Sorgjerd, K., Klingstedt, T., Lindgren, M., Kagedal, K., and Hammarstrom, P. (2008) *Biochemical and biophysical research communications* **377**, 1072-1078
29. Bucciantini, M., Giannoni, E., Chiti, F., Baroni, F., Formigli, L., Zurdo, J., Taddei, N., Ramponi, G., Dobson, C. M., and Stefani, M. (2002) *Nature* **416**, 507-511

30. Kazlauskaite, J., Young, A., Gardner, C. E., Macpherson, J. V., Venien-Bryan, C., and Pinheiro, T. J. (2005) *Biochemical and biophysical research communications* **328**, 292-305
31. Masel, J., Genoud, N., and Aguzzi, A. (2005) *Journal of molecular biology* **345**, 1243-1251
32. Eghiaian, F., Daubenfeld, T., Quenet, Y., van Audenhaege, M., Bouin, A. P., van der Rest, G., Grosclaude, J., and Rezaei, H. (2007) *Proceedings of the National Academy of Sciences of the United States of America* **104**, 7414-7419
33. Gerber, R., Voitchovsky, K., Mitchel, C., Tahiri-Alaoui, A., Ryan, J. F., Hore, P. J., and James, W. (2008) *Journal of molecular biology* **381**, 212-220
34. Hornemann, S., Christen, B., von Schroetter, C., Perez, D. R., and Wuthrich, K. (2009) *The FEBS journal* **276**, 2359-2367
35. Almstedt, K., Nyström, S., Nilsson, K., and Hammarström, P. (2009) *Prion* **3**
36. John, D. M., and Weeks, K. M. (2000) *Protein Sci* **9**, 1416-1419
37. Swietnicki, W., Petersen, R. B., Gambetti, P., and Surewicz, W. K. (1998) *The Journal of biological chemistry* **273**, 31048-31052
38. Kelly, S. M., Jess, T. J., and Price, N. C. (2005) *Biochimica et biophysica acta* **1751**, 119-139
39. Diaz-Espinoza, R., and Soto, C. (2012) *Nature structural & molecular biology* **19**, 370-377
40. DeMarco, M. L., and Daggett, V. (2004) *Proceedings of the National Academy of Sciences of the United States of America* **101**, 2293-2298
41. Govaerts, C., Wille, H., Prusiner, S. B., and Cohen, F. E. (2004) *Proceedings of the National Academy of Sciences of the United States of America* **101**, 8342-8347
42. Smirnovas, V., Baron, G. S., Offerdahl, D. K., Raymond, G. J., Caughey, B., and Surewicz, W. K. (2011) *Nature structural & molecular biology* **18**, 504-506
43. Sigurdson, C. J., Nilsson, K. P., Hornemann, S., Manco, G., Polymenidou, M., Schwarz, P., Leclerc, M., Hammarstrom, P., Wuthrich, K., and Aguzzi, A. (2007) *Nature methods* **4**, 1023-1030
44. Apetri, A. C., Vanik, D. L., and Surewicz, W. K. (2005) *Biochemistry* **44**, 15880-15888
45. Hosszu, L. L., Tattum, M. H., Jones, S., Trevitt, C. R., Wells, M. A., Waltho, J. P., Collinge, J., Jackson, G. S., and Clarke, A. R. (2010) *Biochemistry* **49**, 8729-8738
46. Liemann, S., and Glockshuber, R. (1999) *Biochemistry* **38**, 3258-3267
47. Luhrs, T., Zahn, R., and Wuthrich, K. (2006) *Journal of molecular biology* **357**, 833-841
48. Antonyuk, S. V., Trevitt, C. R., Strange, R. W., Jackson, G. S., Sangar, D., Batchelor, M., Cooper, S., Fraser, C., Jones, S., Georgiou, T., Khalili-Shirazi, A., Clarke, A. R., Hasnain, S. S., and Collinge, J. (2009) *Proceedings of the National Academy of Sciences of the United States of America* **106**, 2554-2558
49. Cobb, N. J., Sonnichsen, F. D., McHaourab, H., and Surewicz, W. K. (2007) *Proceedings of the National Academy of Sciences of the United States of America* **104**, 18946-18951
50. Hafner-Bratkovic, I., Bester, R., Pristovsek, P., Gaedtke, L., Veranic, P., Gaspersic, J., Mancek-Keber, M., Avbelj, M., Polymenidou, M., Julius, C., Aguzzi, A., Vorberg, I., and Jerala, R. (2011) *The Journal of biological chemistry* **286**, 12149-12156
51. Cordeiro, Y., Machado, F., Juliano, L., Juliano, M. A., Brentani, R. R., Foguel, D., and Silva, J. L. (2001) *The Journal of biological chemistry* **276**, 49400-49409
52. Deleault, N. R., Harris, B. T., Rees, J. R., and Supattapone, S. (2007) *Proceedings of the National Academy of Sciences of the United States of America* **104**, 9741-9746

53. Silva, J. L., Lima, L. M., Foguel, D., and Cordeiro, Y. (2008) *Trends in biochemical sciences* **33**, 132-140
54. Silva, J. L., Vieira, T. C., Gomes, M. P., Bom, A. P., Lima, L. M., Freitas, M. S., Ishimaru, D., Cordeiro, Y., and Foguel, D. (2010) *Accounts of chemical research* **43**, 271-279
55. Vieira, T. C., Reynaldo, D. P., Gomes, M. P., Almeida, M. S., Cordeiro, Y., and Silva, J. L. (2011) *Journal of the American Chemical Society* **133**, 334-344
56. Margalith, I., Suter, C., Ballmer, B., Schwarz, P., Tiberi, C., Sonati, T., Falsig, J., Nystrom, S., Hammarstrom, P., Aslund, A., Nilsson, K. P., Yam, A., Whitters, E., Hornemann, S., and Aguzzi, A. (2012) *The Journal of biological chemistry* doi: 10.1074/jbc.M112.355958
57. Hammarstrom, P., Wiseman, R. L., Powers, E. T., and Kelly, J. W. (2003) *Science* **299**, 713-716
58. Johnson, S. M., Connelly, S., Fearns, C., Powers, E. T., and Kelly, J. W. (2012) *Journal of molecular biology* doi: 10.1016/j.jmb.2011.12.060
59. Koh, E., Kim, T., and Cho, H. S. (2006) *Bioinformatics (Oxford, England)* **22**, 297-302
60. Richmond, T. J. (1984) *Journal of molecular biology* **178**, 63-89
61. Richards, F. M. (1977) *Annual review of biophysics and bioengineering* **6**, 151-176

**ACKNOWLEDGEMENTS**
The pRSET A plasmids containing the HuPrP variants were a kind gift from Kurt Wüthrich. We thank Lars-Göran Mårtensson for assistance in analyzing structural data.
**FOOTNOTES**
This work was supported by the EU-FP7 Health programme project LUPAS (AA, PH, PN, SH, SN), the Swedish Research Council (PH), Knut and Alice Wallenberg Foundation (PH, PN), The Swedish Foundation for Strategic Research (PH, PN), Linköping University Center for Neuroscience (RM), A generous gift from Astrid and Georg Olsson is gratefully acknowledged. PH is a Swedish Royal Academy of Science Research Fellows sponsored by a grant from the Knut and Alice Wallenberg Foundation.

The abbreviations used are: 129M/A/V/P/L/W/E/K/C, human prion protein sequence 90-231, carrying substitutions at position 129. Being methionine (M), alanine (A), valine (V), proline (P), leucine (L), tryptophan (W), glutamic acid (E), lysine (K) or cysteine (C); GuHCl, guanidine hydrochloride; $HuPrP_{121-231}$, human prion protein sequence 121-231, $HuPrP_{90-231}$, human prion protein sequence 90-231; HuPrP, human prion protein; ThT, Thioflavin T.

**FIGURE LEGENDS**

**Figure 1. Secondary structure analysis by circular dichroism.**
a) Far UV-circular dichroism spectra of native $HuPrP_{90-231}$, 129-mutants at 4 °C. Color code for mutant identification is shown as inset.
b) Thermal unfolding curves of 129-mutants monitored at 222 nm. Color code as in Fig 1a). Dashed spectrum shows the thermal unfolding curve of $HuPrP_{121-231}$129M.
c) Far UV-circular dichroism spectra of 129-mutants at 4 °C before ( ── ) and after ( - - ) one thermal unfolding cycle.

**Figure 2. Amyloid fibril formation of $HuPrP_{90-231}$ mutants.**
a) Micrographs of Congo red stained aggregates of $HuPrP_{90-231}$, 129-mutants formed under native conditions in 2 mL cryotubes. With open (left image) and crossed polarizers (right image). Scale bar shows 10 µm. All mutants except for 129C displayed Congored birefringence. A side by side overview comparison at lower magnification of 129M and 129C is shown in the lower panel to highlight the lack of Congo red stained aggregates from 129C.
b) Thioflavin T fluorescence spectra of aggregates of $HuPrP_{90-231}$, 129-mutants formed under native conditions. Color code shown as inset. The dashed spectrum shows the fluorescence for native $HuPrP_{90-231}$ in the presence of ThT.

**Figure 3. Non-reduced denaturing SDS-PAGE of 129C and 129M variants**
Samples taken at different time points during the fibril formation reaction, were boiled in non-reducing SDS loading buffer and run on 18% PAGE gels using SDS buffer and the gel was stained with Coomassie. The 129C mutant shows the presence of a 35 kDa band (dimer) that increases over time as the 17.5 kDa band (monomer) decreases. For the 129M variant only the PrP monomer was detected at all time points. The image presented is a composite from duplicate samples run on the same gel (as indicated by dashed lines).

**Figure 4. Amyloid fibril formation kinetics of $HuPrP_{90-231}$ mutants.**
a) Normalized kinetic traces (ThT) of amyloid fibril reactions for all investigated mutants monitored for 24 hours in 96 well plates. Spontaneous reactions displayed in red and the reaction seeded with 1% fibrils displayed in black. The kinetic traces of 129C have been related to the intensity of the wild type (129M) reaction (note the different y-axis). The inset in the 129C graph shows the kinetics of 129C seeded with 1% 129M fibrils. n=6 for each reaction.
b) Amyloid fibril formation kinetic parameters of $HuPrP_{90-231}$ variants, in absence and presence of 1% seed from Fig 4a) (data for 129C not shown). The top panels show lag times and growth rates of the spontaneous reactions and the bottom panels show the same parameters for fibrillation reactions seeded with 1% fibrils from the same sequence. The average lag times and growth rates were calculated for samples that converted within 24 h.
Color code for mutant identification shown at the bottom of the Figure. The insets in the bottom panels show the differences (Δ) of lag time and growth rates compared to spontaneous reactions.

**Figure 5. Schematic mechanisms and kinetics of PrP fibril formation evaluated by amino acid substitutions in position 129**
i) Spontaneous fibrillation in the general case. Native HuPrP (position 129 marked in gray) forms a native dimer (1) which is further converted into a fibrillation competent misfolded oligomeric aggregate (2). This conformational rearrangement is stabilized by intermolecular interactions and exposes different surface amino acids than the native protein. The protein further converts into fibrillation nuclei (3) and fibril elongation is initiated (4), followed by fibril fragmentation (5) in the exponential growth phase.
ii) Seeded reaction. The fibrillation nuclei can directly recruit and convert monomers into the fibrillar state (6).
iii) In the case of 129K, marked in orange, the recruitment of native monomer to the nuclei is abrogated by positive-charge repulsion caused by charged residues exposed on the surface of the fibrillation competent conformation. The seeding mechanism is distorted. The spontaneous reaction is also to some extent delayed by positive charge repulsion (7).
iv) For 129C the formation of a native dimer enables intermolecular covalent disulfide formation (8) and conversion into fibrillation competent conformation is blocked.

**Figure 6 A putative dimerization interface of β–strand 1**
The structure of HuPrP121-231, highlighting β–strand 1 sequence 127-131 (in red) with an intermolecular distance of 3.9 Å between neighbouring 129M residues was recently shown by X-ray crystallography The

interface was revealed as a crystal packing interaction (48). Locking the antiparallell configuration of β–strands 1 and 1' by a disulphide bond in 129C dimer results in a non-convertable state. The structure was drawn using the program PyMol using the coordinates 2W9E from pdb.

Table 1

Conformational stability and properties of $HuPrP_{90-231}$ mutants.

| HuPrP mutant | Tm (°C)[a)] | ΔTm (°C)[b)] | Loss of α-helix % [c)] | Accessible non-polar surface area [d)] |
|---|---|---|---|---|
| 129M | 65.6±0.4 | 0 | 12 | 125.0 |
| 129A | 62.4±0.5 | -3.1 | 12 | 80.4 |
| 129V | 66.1±0.4 | 0.6 | 9 | 127.1 |
| 129L | 65.8±0.4 | 0.3 | 10 | 156.0 |
| 129P | 58.4±0.6 | -7.2 | 15 | Nd |
| 129W | 61.5±0.4 | -4.1 | 21 | 177.2 |
| 129E | 61.2±0.4 | -4.4 | 15 | 57.0 |
| 129K | 66.2±0.3 | 0.7 | 8 | 109.3 |
| 129C | 65.7±0.4 | 0.1 | 30 | 47.4 |
| $HuPrP_{121-231}$129M | 65.3±0.2 | -0.3 | 11 | Na |
| H187R | 53.2±0.6 | -12.3 | 27 | Na |
| F198S | 48.6±0.3 | -17.0 | 17 | Na |

[a)] Midpoint of thermal denaturation measured by far UV circular dichroism at 222 nm.
[b)] Difference in midpoint of thermal denaturation in comparison to 129M (wt)
[c)] Based on change in mean residue ellipticity measured by far UV circular dichroism at 222 nm before and after one round of thermal denaturation 4-90 °C.
[d)] Data referring to the substituted amino acid obtained from Koh et al,(59) which calculated water-accessible non-polar surface areas ($Å^2$) of the side chains in the fully extended β-form of the peptide Gly-X-Gly, by using the Richmond algorithm (60) and van der Waals radii of Richards (61)

Table 2
Tinctorial properties of $HuPrP_{90-231}$ amyloid fibrils

| HuPrP mutant | CR [a] | ThT [b] |
|---|---|---|
| | +/- | Intensity, % of wt |
| 129M | + | 100 ± 30 |
| 129A | + | 90 ± 20 |
| 129V | + | 80 ± 10 |
| 129L | + | 140 ± 40 |
| 129P | + | 150 ± 20 |
| 129W | + | 40 ± 20 |
| 129E | + | 90 ± 20 |
| 129K | + | 170 ± 20 |
| 129C | - | 10 ± 20 |

[a] Congo red birefringence in crossed polarized light microscopy of fibrils formed after 24h.
[b] ThT fluorescence intensity relative to 129M (wt) set to 100%, using a fluorescence plate reader of fibrils formed after 7h in cryo tubes.

Table 3
Kinetic parameters of amyloid fibril formation of $HuPrP_{90-231}$ under near physiological conditions assessed by ThT fluorescence.
*All data are means of 6 trajectories with standard deviations. The trajectories were fitted according to Almstedt et al.(35).*

| HuPrP mutant | lag time (h) | growth rate (h-1) | Conversion ratio[a)] |
|---|---|---|---|
| 129M unseeded | 4,6 ± 1,1 | 0,37 ± 0,14 | 6/6 |
| 129M seeded | 1,5 ± 0,2 | 0,44 ± 0,09 | 6/6 |
| 129A unseeded | 5,3 ± 0,9 | 0,38 ± 0,13 | 6/6 |
| 129A seeded | 1,6 ± 0,3 | 0,28 ± 0,03 | 6/6 |
| 129V unseeded | 5,3 ± 1,6 | 0,11 ± 0,06 | 6/6 |
| 129V seeded | 2,9 ± 1,0 | 0,11 ± 0,02 | 6/6 |
| 129L unseeded | 5,4 ± 2,0 | 0,17 ± 0,03 | 6/6 |
| 129L seeded | 2,4 ± 0,1 | 0,13 ± 0,02 | 6/6 |
| 129P unseeded | 11,8 ± 8,01 | 0,22 ± 0,06 | 4/6 |
| 129P seeded | 2,6 ± 0,5 | 0,24 ± 0,18 | 6/6 |
| 129W unseeded | 14,7 ± 2,1 | 0,10 ± 0,03 | 6/6 |
| 129W seeded | 2,2 ± 0,2 | 0,54 ± 0,06 | 6/6 |
| 129E unseeded | 10,3 ± 1,0 | 0,14 ± 0,07 | 6/6 |
| 129E seeded | 3,4 ± 0,7 | 0,13 ± 0,02 | 6/6 |
| 129K unseeded | 8,3 ± 0,3 | 0,11 ± 0,05 | 3/6 |
| 129K seeded | 10,4 ± 2,4 | 0,15 ± 0,06 | 6/6 |
| 129C unseeded | >24h | n.d. | 0/6 |
| 129C seeded | >24h | n.d. | 0/6 |
| 129C seeded with wt | 2,6 ± 0,7 | 0,15 ± 0,02 | 6/6 |

[a)] Samples/total number of samples that displayed ThT fluorescence within 24 h.

1

a

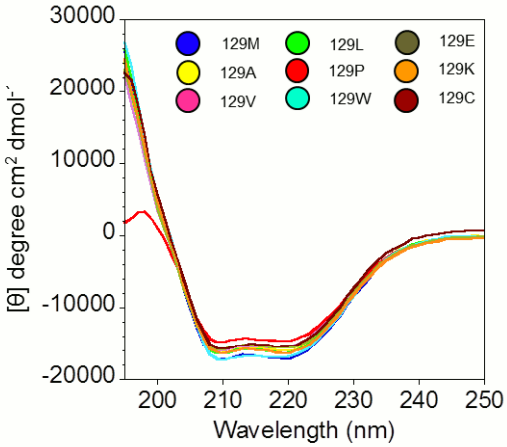


b

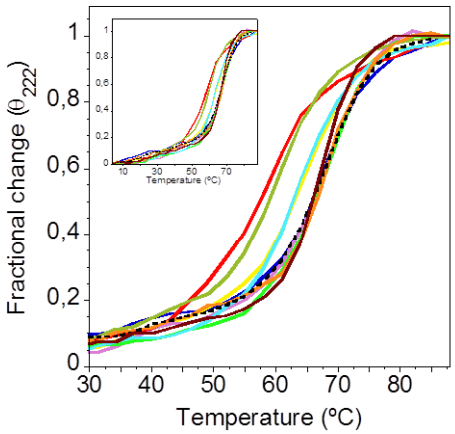


c

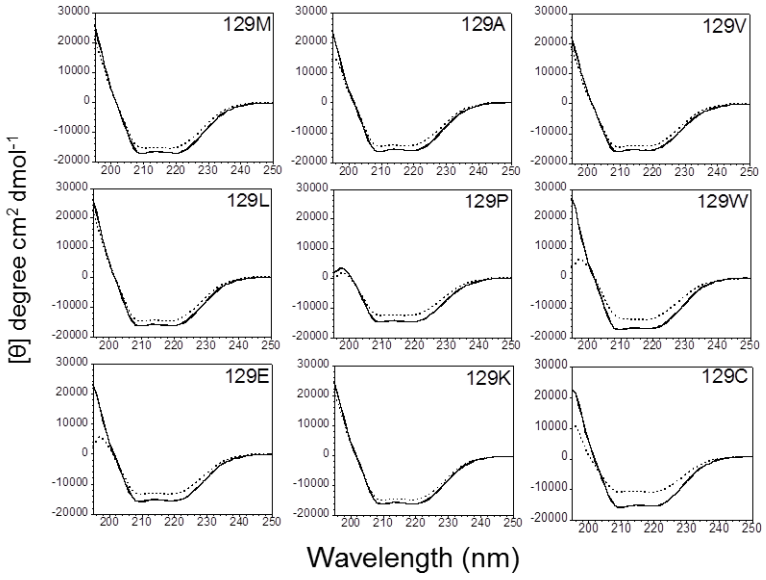


Nyström et al 2012

2

a

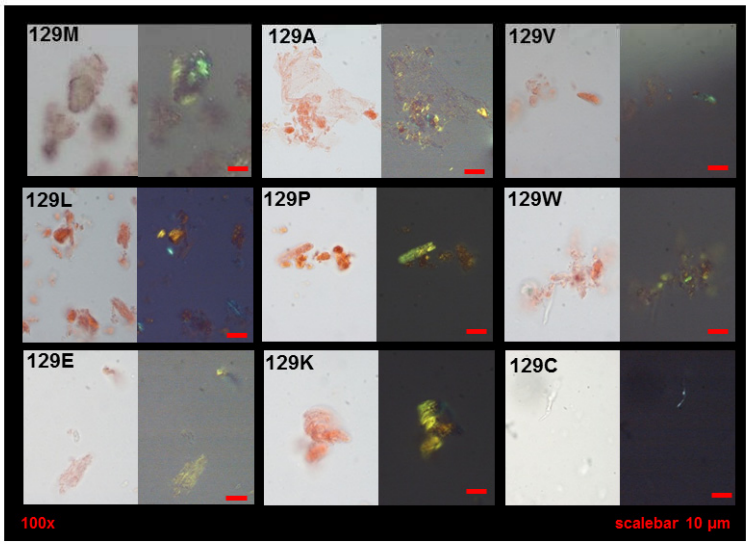


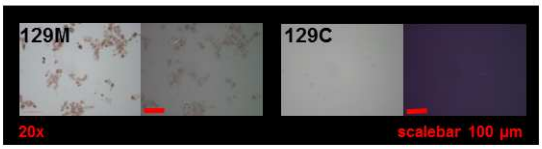


b

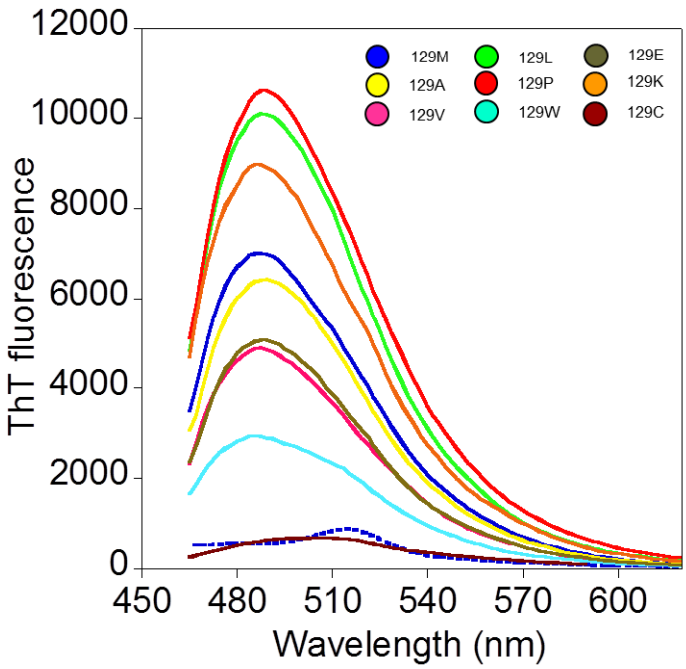


Nyström et al 2012

3

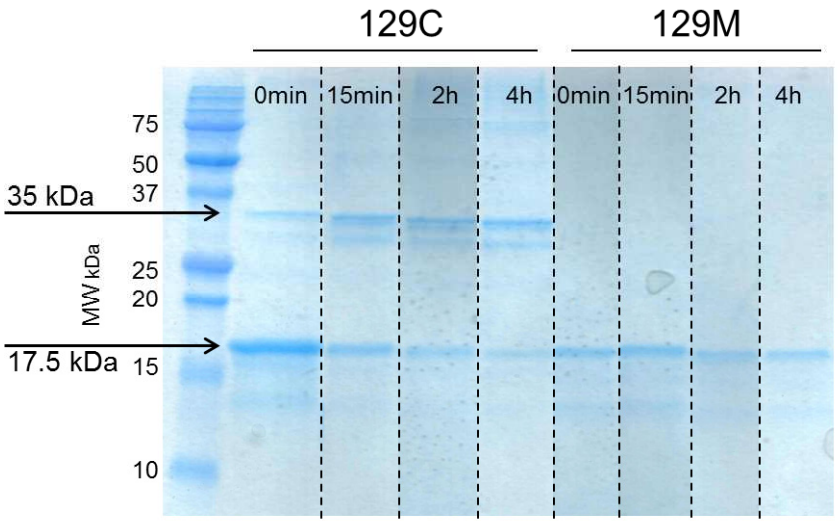




Nyström et al 2012

4

a

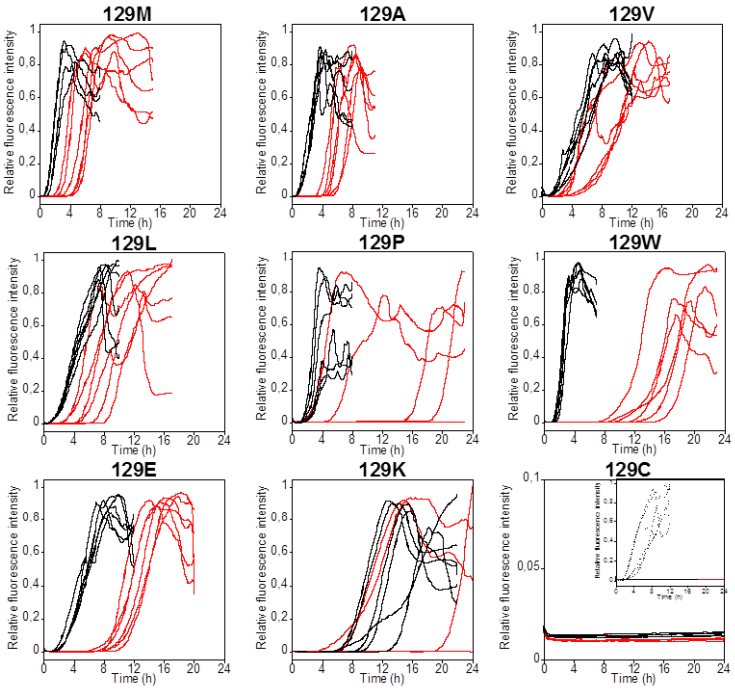


b

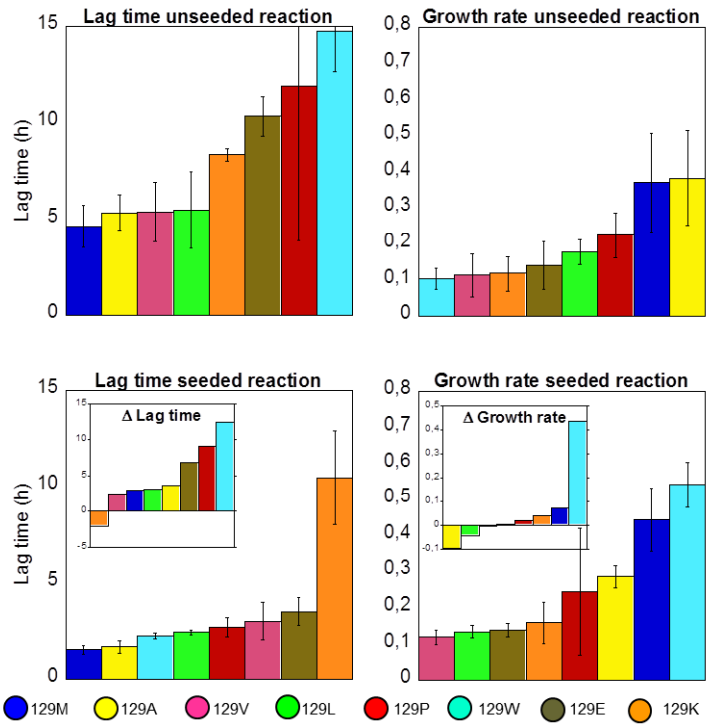

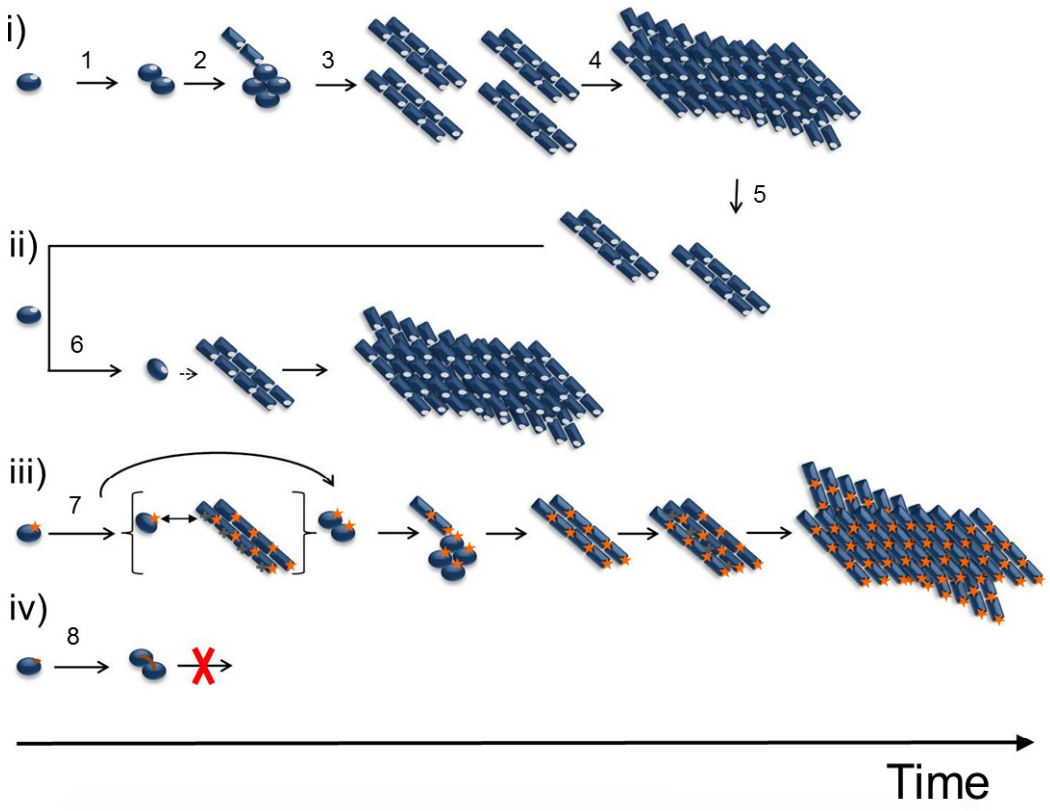




Nyström et al 2012